J Appl Electrochem (2010) 40:631–637
DOI 10.1007/s10800-009-0038-5

ORIGINAL PAPER

Electrochemical corrosion behavior of Al7075 rotating disc electrode in neutral solution containing L-glutamine as a green inhibitor

H. Ashassi-Sorkhabi · E. Asghari

Received: 23 May 2009 / Accepted: 23 November 2009 / Published online: 3 December 2009

Abstract This is a study of the electrochemical corrosion behavior of aluminum alloy Al7075 and its corrosion inhibition using L-glutamine in 3.5% NaCl solution under different hydrodynamic conditions. The hydrodynamic conditions were simulated by using a rotating disc electrode. The results showed that an increase in rotation speed leads to a higher corrosion current density, while the charge transfer resistance decreases and corrosion potential shifts toward more positive values. The inhibition efficiency depends on rotation speed. That is, the efficiency was low in stagnant solution, but enhanced significantly under hydrodynamic conditions. The phenomenon was attributed to the increased mass transport of inhibitor's molecules to the electrode surface that is advantageous for improvement of inhibition efficiency. However, higher rotation speeds ($\Omega \geq 1{,}500$ rpm) cause a slight reduction of efficiency due to higher shear stresses.

Keywords Hydrodynamic · Corrosion · Inhibition · Aluminum · Glutamine

1 Introduction

Since aluminum alloys hold variety of advantages such as favorable strength-to-weight ratio, low density, high electrical and thermal conductivity besides their low price, they are used in a wide range of industries such as manufacturing automobiles, containers, household appliances, electronic devices, batteries, reaction vessels and pipes [1–6]. Owing to their high strength, due to the heterogeneous microstructure based on Al–Zn–Mg–Cu system, the 7xxx series alloys have also found their ways to some widespread uses in different applications especially in aerospace industry [7]. Al7075 alloy with its ultra high strength, compared to the others, which makes it the most suitable material for different parts in highly stressed structures, is widely used for several different applications [8].

Aluminum and its alloys can be protected from corrosion using corrosion inhibitors. Organic or inorganic compounds might be used as inhibitors. Inorganic compounds are mostly toxic and cause severe environmental hazards. Therefore, nowadays the researchers are focusing on non-toxic organic compounds. Environmentally friendly organic compounds that have heteroatoms, including oxygen, sulphur and nitrogen, or heterocyclic compounds containing functional groups and conjugated double bonds are being applied as corrosion inhibitors for different metals [9–16]. For example, ethoxylated fatty acids [17], surfactants [18], tartarate ions [19], vanillin and opuntia extract [9, 12], amino acids [8, 20] and hydroxyl carboxylic acids [8] are used as organic corrosion inhibitors for aluminum and its alloys. Amino acids are amongst the most important compounds that are biodegradable and environmentally friendly and meet some of the environmental regulations [8, 21]. It has been proven that organic compounds establish their inhibition via adsorption of their molecules on metal surface or on oxide films and forming a protective layer [22–27].

Moreover, aluminum alloys have an inclination to flow-assisted-corrosion (FAC) and erosion–corrosion (E–C) in different mediums such as automotive cooling systems, marine conditions, etc. [28]. Thus, the hydrodynamic properties of a solution are important factors affecting corrosion or corrosion inhibition of the alloys. However,

H. Ashassi-Sorkhabi (✉) · E. Asghari
Electrochemistry Research Laboratory, Physical Chemistry Department, Faculty of Chemistry, University of Tabriz, Tabriz, Iran
e-mail: habib_ashassi@yahoo.com; ashassi@tabrizu.ac.ir

there exist few studies published in literatures on the effect of fluid flow on corrosion of aluminum alloys. Niu and Cheng [5] used Al3003 rotating disc electrode to study the E–C of aluminum in ethylene glycol–water mixtures and synergistic effects of fluid flow and sand particles. They observed that in the absence of sand particles, an increase in rotation speed leads to an acceleration in oxygen diffusion and an increase of cathodic current density. At the same time, aluminum is oxidized to form an oxide film leading to a decreased anodic current density. They also found that at low and intermediate electrode rotation speeds, the electrode process occurring on aluminum alloy surface is controlled by both activation and diffusion steps. However, at higher rotation speeds the electrode process is largely dominated by the activation control. Xu and Cheng [28] also studied the FAC of an aluminum alloy in ethylene glycol–water solution by using an impingement jet system.

Rosliza et al. [6] studied corrosion inhibition of Al6061 alloy in tropical seawater while using sodium benzoate under static and air circulation conditions. They observed that, compared to static conditions, the air circulation increased corrosion rate of Al6061 alloy. However, in the presence of inhibitor, this enhancement was significantly lesser. Pyun and Moon [29] also investigated the mechanism of corrosion of pure aluminum in alkaline solution under stagnant and stirred conditions.

Because of the importance of flow effects on corrosion and corrosion inhibition of aluminum alloys and due to lack of adequate studies in this field, the present work's aim is to investigate the effect of hydrodynamic conditions on corrosion of Al7075 alloy in neutral solution. The corrosion inhibition of this alloy is also studied by using an amino acid, L-glutamine, under different hydrodynamic conditions. The hydrodynamic conditions have been simulated by using an Al7075 rotating disc electrode. The electrochemical techniques including polarization and electrochemical impedance spectroscopy (EIS) have been performed for the corrosion studies.

2 Experimental

Electrochemical tests were performed through conventional three-electrodes configuration: a Pt rod as counter electrode, an Ag/AgCl (3 M KCl) as reference electrode and an Al7075 rotating disc electrode (RDE) with chemical composition (wt%) of Zn: 5.5, Mg: 2.1, Cu: 1.5, Fe: 0.5, Si: 0.4, Mn: 0.3, Ti: 0.2, Cr: 0.2 and Al balance, as working electrode. The Al7075 bar was fully mounted in a polyester resin in such a way that only the end surface remained exposed with a surface area of 0.283 cm^2 ($Ø = 6$ mm). This assembly was machined to form a rotating disc electrode. Just before each test, the working electrode was polished by SiC papers up to 1200 grade. Then, it was dipped in a 4:1 (v/v) mixture of HNO_3 (65%) and distilled water for one minute. Finally, the sample was degreased with ethanol and rinsed with distilled water. The electrolyte used for corrosion studies was a 3.5% NaCl solution and the inhibitor was L-glutamine (H_2N–(CO)–$(CH_2)_2$–$CH(NH_2)$–COOH) produced by Merck Company. The tests were performed at static conditions with three different concentrations (5×10^{-4}, 1×10^{-3} and 5×10^{-3} M) of inhibitor. The concentration of 5×10^{-3} M showed the highest inhibition efficiency. So, this concentration was selected for further experiments under different hydrodynamic conditions. The solution volume was fixed at 100 mL and the temperature was 25 ± 1 °C in all experiments.

To perform the polarization and electrochemical impedance spectroscopy (EIS) measurements the Autolab PGSTAT30 potentiostat–galvanostat and frequency response analyzer (FRA) were used. An AFMSRX rotator, manufactured by PINE Instruments Company, was used to control the rotation speed of RDE.

In order to obtain a steady state open circuit potential, the electrode was immersed in the test solution for 60 min. Immediately after this period of time, the EIS tests were performed over a frequency range between 1 and 10 MHz using a ±10 mV (rms) sinusoidal potential perturbation in open circuit potential. The EIS data were analyzed by using Zview2 software and fitted to an appropriate equivalent circuit model. All electrochemical experiments were repeated for three times to assure the reproducibility of the data and the results.

The anodic branches of polarization curves were obtained by sweeping the potential towards the anodic direction with a scan rate of 2 mV s^{-1}. The initial potential was −0.7 V vs. Ag/AgCl that was slightly cathodic with respect to open circuit potential.

3 Results and discussions

3.1 Polarization measurements

Figure 1 represents typical anodic polarization curves for corrosion of Al7075 RDE in blank and inhibited solutions under different hydrodynamic conditions. The corrosion current densities were obtained from these curves [30]. The obtained parameters including corrosion current density, i_{corr}, corrosion potential, E_{corr}, and inhibition efficiency at each electrode rotation rate are presented in Table 1. The Reynolds numbers, Re, are also calculated using following equation [31] and given in Table 1.

$$\mathrm{Re} = \frac{r^2 \cdot \omega}{\kappa_\upsilon} \quad < 10^5 \text{ for laminar flow} \tag{1}$$

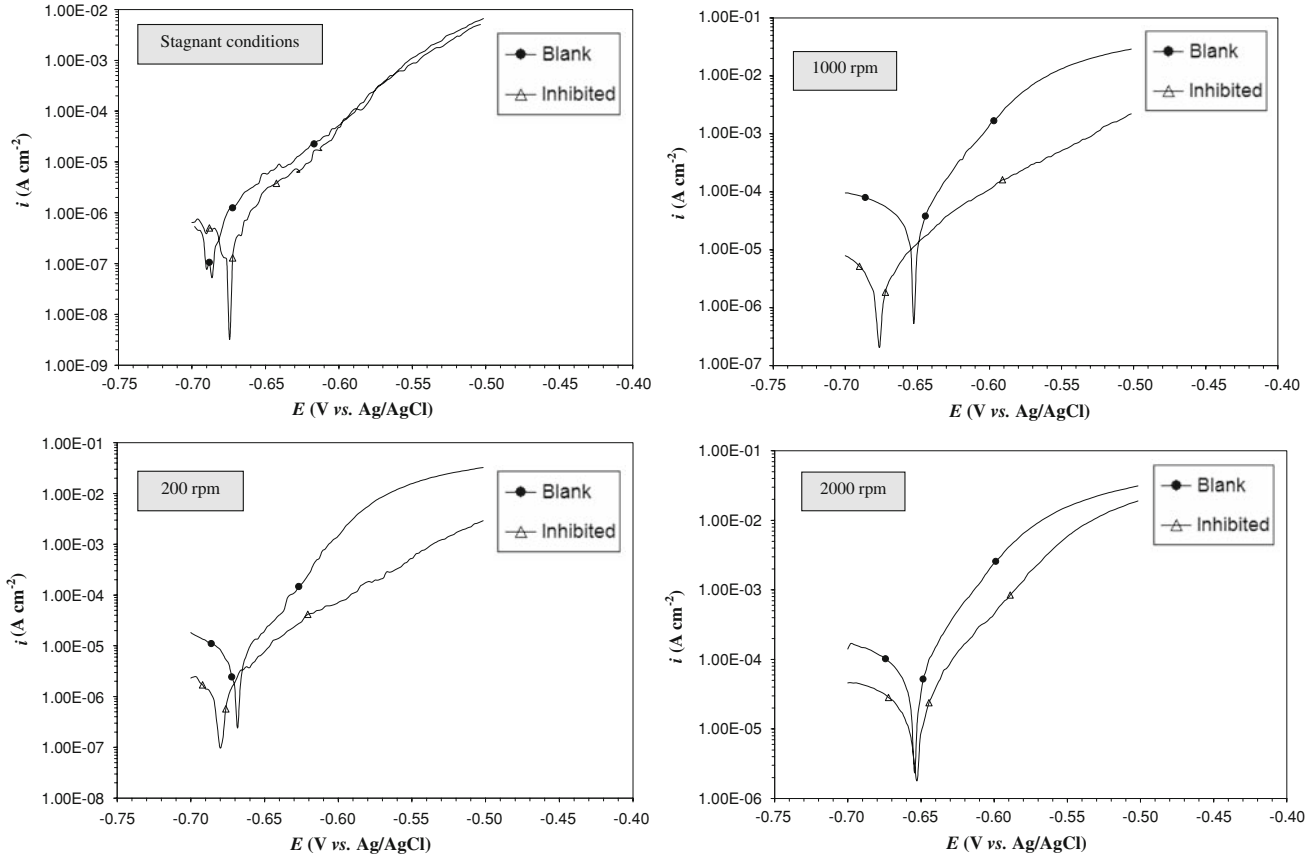

Fig. 1 Typical anodic polarization curves for Al7075 RDE under stagnant conditions and some rotation speeds

Table 1 Electrochemical parameters for dissolution of Al7075 in the absence and presence of L-glutamine in 3.5% NaCl at different rotation speeds and the Reynolds numbers corresponding to each rotation rate

Rotation rate (rpm)	Reynolds numbers	i_{corr} (μA cm^{-2})	E_{corr} (V/Ag–AgCl)	η_p%
3.5% NaCl				
0	0	0.6	−0.68	–
200	843.4	4.0	−0.67	–
500	2108.5	13.0	−0.66	–
1,000	4217	45.0	−0.65	–
1,500	6325.5	90.3	−0.65	–
2,000	8,434	102.0	−0.65	–
3.5% NaCl + glutamine				
0	0	0.3	−0.67	50.0
200	843.4	1.0	−0.68	75.0
500	2108.5	3.0	−0.67	76.9
1,000	4,217	6.1	−0.68	86.7
1,500	6325.5	14.2	−0.66	84.3
2,000	8,434	28.0	−0.65	72.5

where r, ω and κ_v are the radius of the RDE active area in mm, angular velocity in rad/s and kinematics viscosity in stokes (mm^2/s), respectively. The Reynolds numbers show that the flow is laminar in the all studied rotation speeds.

The inhibition efficiencies, η_p%, are calculated using the following equation [32]:

$$\eta_p\% = \left(\frac{i^o_{corr} - i_{corr}}{i^o_{corr}}\right) \times 100 \quad (2)$$

where i^o_{corr} and i_{corr} are corrosion current densities in the absence and presence of inhibitor respectively.

It is obvious from Table 1 that E_{corr} has not been significantly affected by the electrode rotation rate. E_{corr} shows only a maximum shift of about 30 mV toward more positive potentials when the electrode rotation speed increases. It is also clear that as the electrode rotates, the i_{corr} increases in several orders of magnitude. This enhancement is more significant at low rotation speeds, but i_{corr} stays at an approximately constant value when high rotation rates are applied.

According to Pourbaix potential-pH diagram of aluminum, when pH is within the range of 4–9, Al is oxidized to form an oxide film on the electrode. Reactions in a neutral solution are characterized by the following equations [5]:

$$\text{Cathodic reaction: } 3/2O_2 + 3H_2O + 6e \rightarrow 6OH^- \quad (3a)$$

$$\text{Anodic reaction: } 2Al + 6OH^- \rightarrow Al_2O_3 + 3H_2O + 6e \quad (3b)$$

The dissolved oxygen diffuses towards Al electrode surface and the oxygen reduction reaction generates hydroxide ions. Consequently, the produced hydroxide ions react with Al to produce aluminum oxide [5].

The fluid flow has its own effects on Al corrosion in the blank solution. These effects are:

(i) Mass transfer of dissolved oxygen (cathodic reactant) from bulk of the electrolyte to the electrode surface increases with the increase of rotation rate.
(ii) The raised supply of cathodic reactant on electrode surface accelerates the cathodic reaction. As a result, more OH^- ions are produced.
(iii) The addition of OH^- ions supply on metal surface moves the reaction (3b) in forward direction. Following this shift, further dissolution of aluminum occurs.
(iv) Shear stresses due to hydrodynamic conditions lead to the separation of some insoluble corrosion products from Al surface.

All of the above-mentioned effects lead to an increase in corrosion rate. Besides, in the presence of the inhibitor some other factors influence the corrosion properties and inhibitor performance.

In comparison to the blank solution, when glutamine is used, corrosion current densities are lower at each rotation speeds (Table 1). It was also observed that inhibition efficiency increases with the increase of rotation rate up to 1,000 rpm, and then decreases for about 10% at higher rotation speeds.

It is well known that most organic inhibitors protect metal from corrosion through adsorption phenomenon; forming a barrier layer between the metal and corrosive electrolyte. It is generally accepted that the first step in the adsorption of an organic inhibitor on a metal surface usually involves the replacement of a number of water molecules adsorbed on the metal surface. Then, the inhibitor molecules form a protective layer on metal surface, so that adsorbed layer protects metal from further corrosion [21, 33]:

$$Inh_{(sol)} + xH_2O_{(ads)} \rightleftarrows Inh_{(ads)} + xH_2O_{(sol)} \quad (4)$$

The inhibition efficiency depends on the mechanical, structural and chemical properties of the said layer. Thus, the nature of the inhibitor interaction with the metal and its inhibition efficiency may also depend on the chemical, mechanical and structural characteristics of this layer [21]. Hydrodynamic conditions can also affect surface protection and inhibition efficiency. Generally, in the presence of inhibitor, two opposite effects for hydrodynamic conditions can be considered, which influence its inhibition performance [34, 35]:

(i) Flow can increase mass transport of inhibitor molecules toward the metal surface and improve the inhibition performance.
(ii) The high shear stress resulting from flow velocity can also lead to desorption of adsorbed inhibitor molecules from the metal surface, which plays a negative role on inhibition efficiency.

The outcome of these two opposite effects determines the manner of the variations in $\eta\%$ with electrode rotation rate.

3.2 EIS studies

Figure 2 exhibits the typical Nyquist plots for corrosion of Al7075 alloy in blank and inhibited solutions under different hydrodynamic conditions. Figure 3 shows the appropriate equivalent circuit to be used to fit data properly. In the circuit, R_s and R_{ct} are the solution and charge transfer resistances respectively, CPE stands for the constant phase element related to the double layer capacitance, W_{sr} represents the finite-diffusion impedance and R_L and C_L stand for the resistance and capacitance related to the low frequency inductive loop, respectively.

In some systems like RDE, there is a region close to the electrode surface in which mass transport occurs only by diffusion being called "Nernst diffusion layer" or NDL [36, 37]. Outside the NDL region, the solution is homogeneous due to the stirring produced by the rotating electrode assembly. The electroactive species simply diffuse through NDL to reach the surface of the electrode. In this case, the Nyquist plots have an asymmetrical shape called "finite length diffusion" [36, 37]. Such an asymmetrical shape was also seen in the Nyquist plots obtained for corrosion of Al7075 in 3.5% NaCl solution at rotation speeds of higher than 500 rpm (Fig. 2a). On the other hand, there is a high frequency depressed capacitive loop in every plot caused by the time constant of the electrical double layer, which is called constant phase element (CPE). The CPE defined by Q and n, is employed in the model to compensate for the inhomogeneities in the electrode surface as depicted by depressed nature of Nyquist semicircle [38]. The CPE is often used to interpret data for rough solid electrodes. The impedance, Z, of the CPE is [38–40]:

$$Z_{CPE} = Q^{-1}(j\omega)^{-n} \quad (5)$$

where Q and n stand for the CPE constant and exponent, respectively, $j = (-1)^{1/2}$ is the imaginary number, and ω is the angular frequency in rad s^{-1} ($\omega = 2\pi f$ when f is the

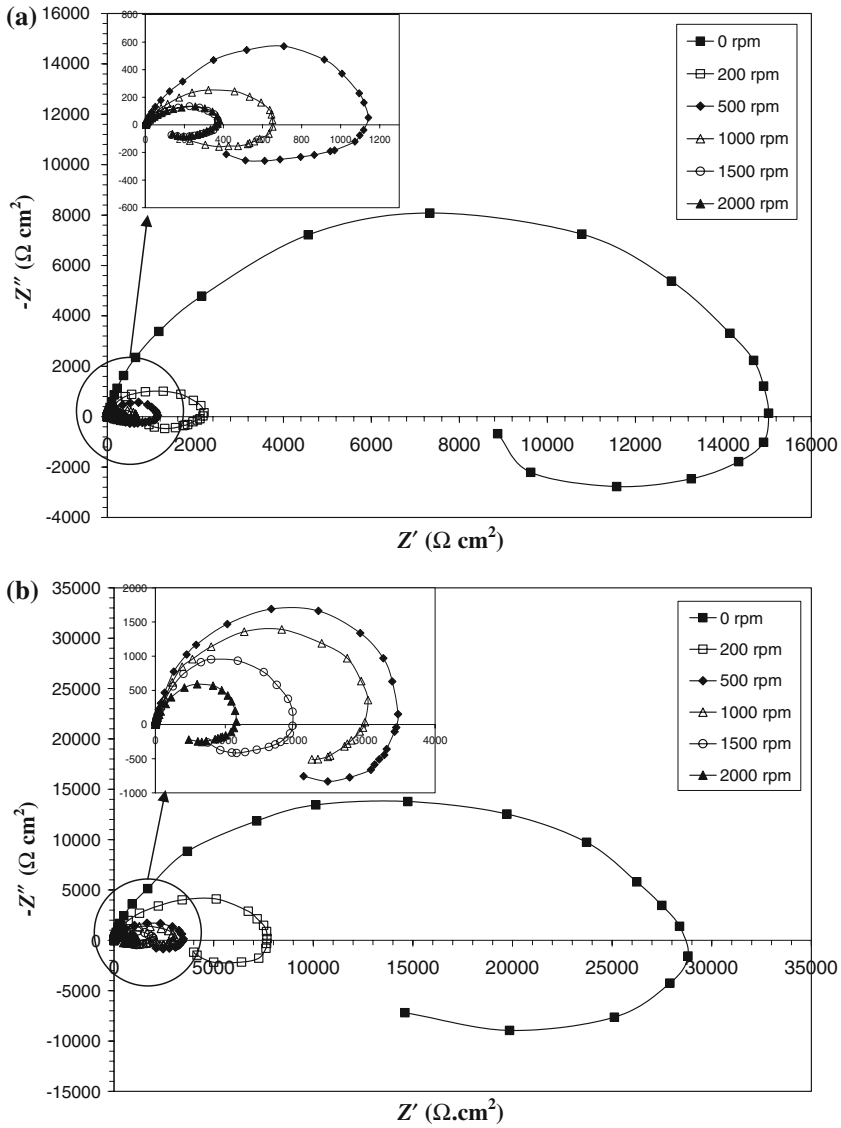

Fig. 2 Typical Nyquist plots for Al7075 RDE in **a** blank and **b** inhibited NaCl solutions under different hydrodynamic conditions

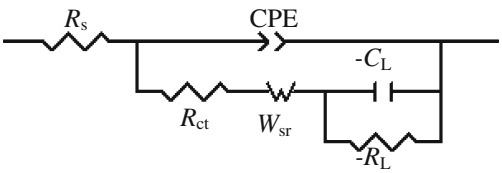

Fig. 3 Electrochemical equivalent circuit for Al7075 RDE in NaCl solution

frequency in Hz). The values of double-layer capacitance, C_{dl}, can be derived from the following equation, at the frequency that the imaginary component of impedance is maximum ($-Z''_{max}$) [41]:

$$f\left(-Z''_{max}\right) = \frac{1}{2\pi C_{dl} R_{ct}} \quad (6)$$

In addition, a low frequency inductive loop was seen in all EIS spectra. Electrochemical reactions often occur at a series of partial reactions, referred to as reaction steps. One or more of the individual steps in a complex reaction may be significantly slower than the others and the slowest step can determine the fastness of the changes in chemical composition of electrical double layer, EDL, responding to polarization voltage magnitude and polarity changes. Restricting changes in EDL chemistry can produce inductance. Adsorption or desorption equilibrium of surface-active species, or corrosion inhibitors, on a metal surface has also been reported as a possible source of induction in EIS spectra [30].

However, in literatures the inductive loop of aluminum has also been attributed to some other phenomena [42]. For example, it has been referred to surface or bulk relaxation of species in the oxide layer [43]. Cinderey and Burstein's measurements [44–47] confirmed that the inductive loop was closely related to the existence of a passive film on

Table 2 Electrochemical impedance parameters for Al7075 corrosion in the absence and presence of glutamine in 3.5% NaCl at different rotation speeds

Rotation speed (rpm)	R_{ct} (Ω cm^2)	$Q \times 10^{-6}$ (Ω^{-1} cm^{-2} s^n)	n	$-R_L$ (Ω cm^2)	$-C_L$ (mF cm^{-2})	W_{sr} (Ω cm^2 s$^{-0.5}$)	η_z%
3.5% NaCl							
0	15979.9	10.6	0.96	6916.5	0.62	–	–
200	2150.8	15.0	0.93	1198.2	3.30	–	–
500	1100.9	24.2	0.89	511.7	14.0	413.6	–
1,000	600.0	45.6	0.83	303.6	23.7	204.3	–
1,500	410.4	120.0	0.75	163.5	47.7	145.9	–
2,000	410.1	121.0	0.75	163.0	48.0	145.0	–
3.5% NaCl + glutamine							
0	28832.0	9.15	0.96	11464.3	0.57	–	44.6
200	7381.2	9.50	0.93	4334.1	1.24	–	70.9
500	3962.0	11.9	0.93	1740.7	4.24	–	72.2
1,000	3205.0	15.0	0.92	1023.0	5.58	–	81.3
1,500	1981.0	15.6	0.93	849.0	6.01	–	79.3
2,000	1301.8	18.7	0.92	522.6	6.23	–	68.5

aluminum. Bessone et al. [48] observed an inductive loop for the pitted active state on aluminum, and attributed the phenomena to surface area modulation or salt film property modulation. Frichet et al. [49] proposed the same hypothesis for the anodic dissolution of aluminum in acidic sodium chloride solution.

The parameters obtained from EIS studies are given in Table 2. It is clear that, the R_{ct} decreases as the electrode rotation speed increases. This observation is in agreement with the increase of i_{corr} along with the increase in rotation rate. A similar trend is observed in the presence of inhibitor. The inhibition efficiencies, η_z%, can also be calculated from R_{ct} values applying the following equation [32]:

$$\eta_z\% = \left(\frac{R_{ct} - R_{ct}^o}{R_{ct}}\right) \times 100 \quad (7)$$

where R_{ct}^o and R_{ct} are charge transfer resistances in the absence and presence of inhibitor, respectively.

Similar to η_p%, the η_z% has also a relatively low value at stagnant conditions but it increases up to 81.3% at 1,000 rpm and then decreases about 10% at higher rotation speeds.

Polarization and EIS measurements lead us to conclude that at quiescence conditions, the adsorption of glutamine molecules on Al surface is relatively low. However, the hydrodynamic conditions facilitate mass transport of inhibitor molecules toward the metal surface. As a result, the aluminum surface protection improves and the inhibition efficiency increases. At speeds higher than 1,000 rpm, high shear stresses on metal surface lead to desorption of some of the adsorbed inhibitor molecules from metal surface and therefore, the inhibition performance reduces.

4 Conclusion

Influence of flow on corrosion and corrosion inhibition of the Al7075 alloy in 3.5% NaCl was studied. It was observed that the corrosion parameters and inhibitor performance depend on the hydrodynamic conditions. When the electrode rotation speed increases, the i_{corr} also increases while the R_{ct} decreases. Their variations were more significant at lower rotation speeds. The inhibition efficiency had a low value at stagnant solution, but increased significantly under hydrodynamic conditions. The enhancement of the efficiency was attributed to the increased mass transport of inhibitor molecules toward the electrode surface. However, there was a reduction of inhibition efficiency at higher speeds. This was ascribed to desorption and separation of surface protective films resulting from high shear stresses at rotation speeds higher than 1,000 rpm. Therefore, the critical electrode rotation rate for the best performance of inhibitor is 1,000 rpm.

Acknowledgements The authors would like to thank Dr. Reza Sadreddini and Er. M. Majid Azar for grammatical revision of the text, Er. M. Rahimi for preparation of Al7075 rotating disc electrodes and University of Tabriz for financial support.

References

1. Liu Y, Sun D, You H, Chung JS (2005) Appl Surf Sci 246:82
2. Fushimi K, Yamamoto S, Ozaki R, Habazaki H (2008) Electrochim Acta 53:2529
3. Li Y, Fedkiw PS (2007) Electrochim Acta 52:2471
4. Sherif EM, Park SM (2006) Electrochim Acta 51:1313
5. Niu L, Cheng YF (2008) Wear 265:367

6. Rosliza R, Senin HB, Wan Nik WB (2008) Colloids Surf A 312:185
7. Birbilis N, Cavanaugh MK, Buchheit RG (2006) Corros Sci 48:4202
8. Bereket G, Yurt A (2001) Corros Sci 43:1179
9. El-Etre AY (2003) Corros Sci 45:2485
10. Monticelli C, Brunoro G, Frignani A, Zucchi F (1991) Corros Sci 32:693
11. Zhu D, Van Ooij WJ (2003) Corros Sci 45:2177
12. El-Etre AY (2001) Corros Sci 43:1031
13. Ashassi-Sorkhabi H, Nabavi-Amri SA (2000) Acta Chim Slov 47:507
14. Ebenso EE, Ekpe UJ, Ita BI, Offiong EO, Ibok UJ (1999) Mater Chem Phys 60:79
15. Ferreria ES, Giacomelli C, Giacomelli FC, Spinelli A (2004) Mater Chem Phys 83:129
16. Saidman SB, Bessone JB (2002) J Electroanal Chem 521:87
17. El-Sherbini EEF, Abd-El-Wahab SM, Deyab MA (2003) Mater Chem Phys 82:631
18. Zhao T, Mu G (1999) Corros Sci 41:1937
19. Shao HB, Wang JM, Zhang Z, Zhang JQ, Cao CN (2002) Mater Chem Phys 77:305
20. Ashassi-Sorkhabi H, Ghasemi Z, Seifzadeh D (2005) Appl Surf Sci 249:408
21. Oguzie EE, Unaegbu C, Ogukwe CN, Okolue BN, Onuchukwu AI (2004) Mater Chem Phys 84:363
22. Bayol E, Gürten T, Gürten AA, Erbil M (2008) Mater Chem Phys 112:624
23. Keleş H, Keleş M, Dehri İ, Serindağ O (2008) Mater Chem Phys 112:173
24. Vishwanatham S, Haldar N (2008) Corros Sci 50:2999
25. Kalman E, Palinkas G (1993) Corros Sci 35:1471
26. Bentiss F, Lagrenee M, Traisnel M, Hornez JC (1999) Corros Sci 41:789
27. Lukovits I, Kalman E, Zucchi F (2001) Corrosion 57:3
28. Xu LY, Cheng YF (2008) Corros Sci 50:2094
29. Pyun SI, Moon SM (2000) J Solid State Electrochem 4:267
30. Tait WS (1994) An introduction to electrochemical corrosion testing for practicing engineers and scientists. ParisODocs, Paris
31. Perez N (2004) Electrochemistry and corrosion science. Kluwer, Massachusetts
32. Es-Salah K, Keddam M, Rahmouni K, Srhiri A, Takenouti H (2004) Electrochim Acta 49:2771
33. Bockris JOM, Swinkels DAJ (1964) J Electrochem Soc 111:736
34. Ashassi-Sorkhabi H, Asghari E (2008) Electrochim Acta 54:162
35. Jiang X, Zheng YG, Ke W (2005) Corros Sci 47:2636
36. Jacobsen T, West K (1995) Electrochim Acta 40:255
37. Billot M, Didierjean S, Lapicque F (2004) J Appl Electrochem 34:1191
38. Nyikos L, Pajkossy T (1985) Electrochim Acta 30:1533
39. Mansfeld F, Kendig MW, Lorenz WJ (1985) J Electrochem Soc 132:290
40. Macdonald JR, Franceschetti DR (1987) In: Macdonald JR (ed) Impedance spectroscopy: emphasizing solid materials and systems. Wiley, New York
41. Kissi M, Bouklah M, Hammouti B, Benkaddour M (2006) Appl Surf Sci 252:4190
42. Metikoš-Huković M, Baić R, Grubač Z (2002) J Appl Electrochem 32:35
43. Freres SE, Stefenel MM, Mayer C, Chierchie T (1990) J Appl Electrochem 20:996
44. Brustein GT, Cinderey RJ (1991) Corros Sci 32:1195
45. Cinderey RJ, Brustein GT (1992) Corros Sci 33:475
46. Cinderey RJ, Brustein GT (1992) Corros Sci 33:493
47. Cinderey RJ, Brustein GT (1992) Corros Sci 33:499
48. Bessone JB, Salinas DR, Mayer C, Ebert M, Lorenz WJ (1992) Electrochim Acta 37:2283
49. Frichet A, Gimenez P, Keddam M (1993) Electrochim Acta 38:1957